Cell Reports
Physical Science

CellPress
OPEN ACCESS

Article

The role of structural defects in commercial lithium-ion batteries

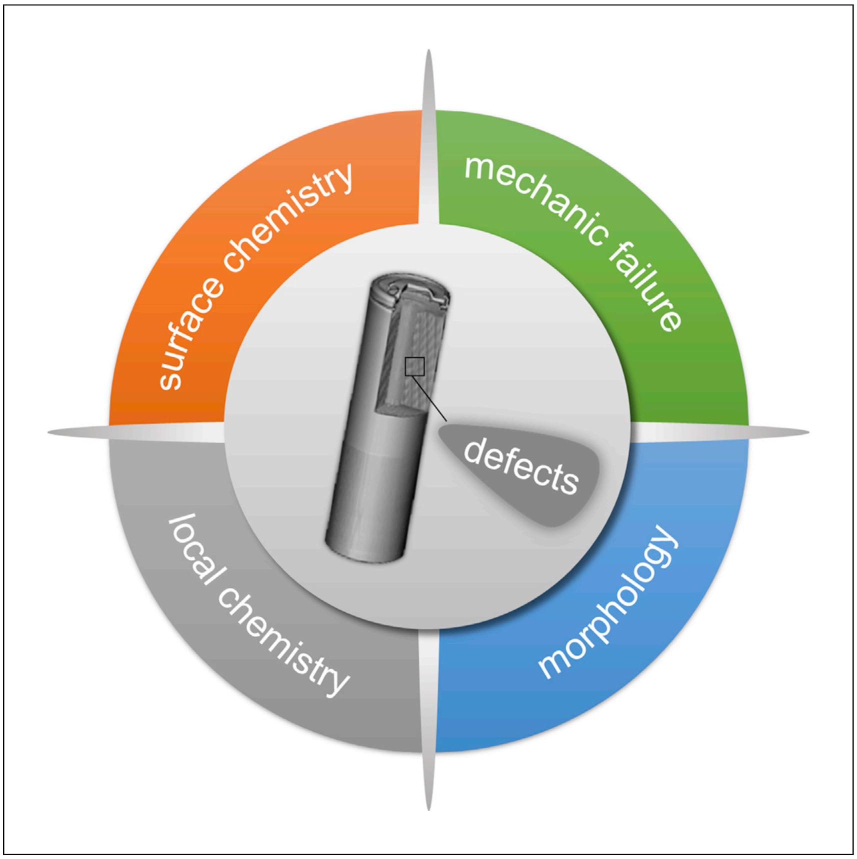

Structural defects in lithium-ion batteries can significantly affect their electrochemical and safe performance. Qian et al. investigate the multiscale defects in commercial 18650-type lithium-ion batteries using X-ray tomography and synchrotron-based analytical techniques, which suggests the possible degradation and failure mechanisms associated with the impurity defects.

Guannan Qian, Federico Monaco, Dechao Meng, ..., Linsen Li, Peter Cloeten, Yijin Liu

xyu@iphy.ac.cn (X.Y.)
linsenli@sjtu.edu.cn (L.L.)
cloetens@esrf.eu (P.C.)
liuyijin@slac.stanford.edu (Y.L.)

Highlights

Multiscale and 3D visualization of structural defects in commercial batteries

Elucidation of the impurity particles' detrimental effects on the battery performance

Functional mechanisms of structural defects in commercial batteries are summarized

Qian et al., Cell Reports Physical Science *2*, 100554
September 22, 2021
https://doi.org/10.1016/j.xcrp.2021.100554

Please cite this article in press as: Qian et al., The role of structural defects in commercial lithium-ion batteries, Cell Reports Physical Science (2021), https://doi.org/10.1016/j.xcrp.2021.100554

Cell Reports
Physical Science

CellPress
OPEN ACCESS

Article

The role of structural defects in commercial lithium-ion batteries

Guannan Qian,[1,2,9] Federico Monaco,[3,9] Dechao Meng,[1,9] Sang-Jun Lee,[2] Guibin Zan,[2] Jizhou Li,[2] Dmitry Karpov,[3] Sheraz Gul,[4] David Vine,[4] Benjamin Stripe,[4] Jin Zhang,[2,5] Jun-Sik Lee,[2] Zi-Feng Ma,[1] Wenbin Yun,[4] Piero Pianetta,[2] Xiqian Yu,[6,7,*] Linsen Li,[1,8,*] Peter Cloeten,[3,*] and Yijin Liu[2,10,*]

SUMMARY

The manufacturing of commercial lithium-ion batteries (LIBs) involves a number of sophisticated production processes. Various cell defects can be induced, and, depending on their structural and chemical characteristics, they could lead to acute failure and/or chronic degradation. Although tremendous efforts have been devoted to develop a robust quality control (QC) procedure, the functional role of the cell defects is not well understood. Here, we address this question through a systematic experimental study of commercial 18650-type LIBs that have failed the QC inspection due to a self-discharging effect. We identify and recover the defective regions from the cell and conduct a comprehensive investigation from the chemical, structural, and morphological perspectives. Our results reveal how the structural defects affect the cell performance, which is highly important to industry-scale battery production.

INTRODUCTION

With its advantages in high energy and power densities, long cycling span, and environmental friendliness, the lithium-ion battery (LIB) has become one of the most promising energy storage configurations for electric vehicles (EVs).[1,2] To meet the requirements in acceleration power and endurance mileage, a large number of LIBs are connected in parallel or in series to constitute a battery pack.[3] Given the high degree of complexity of a battery pack, a dedicated battery management system (BMS) is often used to supervise its state and executive function.[4,5] For example, through a process termed "active equalization,"[6] the BMS proactively coordinates the states of all of the cells in the pack to prevent operating any of the cells at overcharged or insufficiently charged states, which could lead to safety hazard[7–9] or capacity loss,[10] respectively. This approach is crucial to both the safety and the service life of the EVs.

The active equalization method is often model based. The model formulates an electrochemical procedure and applies it to a certain cell based on the measurement of its electric signals.[6] If a certain cell behaves differently from its peers in the same battery pack, the BMS may not recognize this situation because its model does not apply to this defective cell. For example, by treating a defective cell with internal soft shorts as a normal cell, the BMS could further enhance the damage by draining the energy through this cell in a cascade fashion, forming a vicious circle. It is, therefore, critically important to identify defective cells in a LIB assembly line, and this has motivated the development of rigorous quality control (QC) procedures.

[1]Department of Chemical Engineering, Shanghai Electrochemical Energy Device Research Center (SEED), School of Chemistry and Chemical Engineering, Frontiers Science Center for Transformative Molecules, Shanghai Jiao Tong University, Shanghai 200240, China

[2]Stanford Synchrotron Radiation Lightsource, SLAC National Accelerator Laboratory, Menlo Park, CA 94025, USA

[3]ESRF-The European Synchrotron, Grenoble 38043, France

[4]Sigray, Concord, CA 94520, USA

[5]Beijing Synchrotron Radiation Facility, Institute of High Energy Physics, Chinese Academy of Science, Beijing 100049, China

[6]Beijing Advanced Innovation Center for Materials Genome Engineering, Institute of Physics, Chinese Academy of Sciences, Beijing 100190, China

[7]Center of Materials Science and Optoelectronics Engineering, University of Chinese Academy of Sciences, Beijing 100049, China

[8]Shanghai Jiao Tong University Sichuan Research Institute, Chengdu 610213, China

[9]These authors contributed equally

[10]Lead contact

*Correspondence: xyu@iphy.ac.cn (X.Y.), linsenli@sjtu.edu.cn (L.L.), cloetens@esrf.eu (P.C.), liuyijin@slac.stanford.edu (Y.L.)

https://doi.org/10.1016/j.xcrp.2021.100554

Please cite this article in press as: Qian et al., The role of structural defects in commercial lithium-ion batteries, Cell Reports Physical Science (2021), https://doi.org/10.1016/j.xcrp.2021.100554

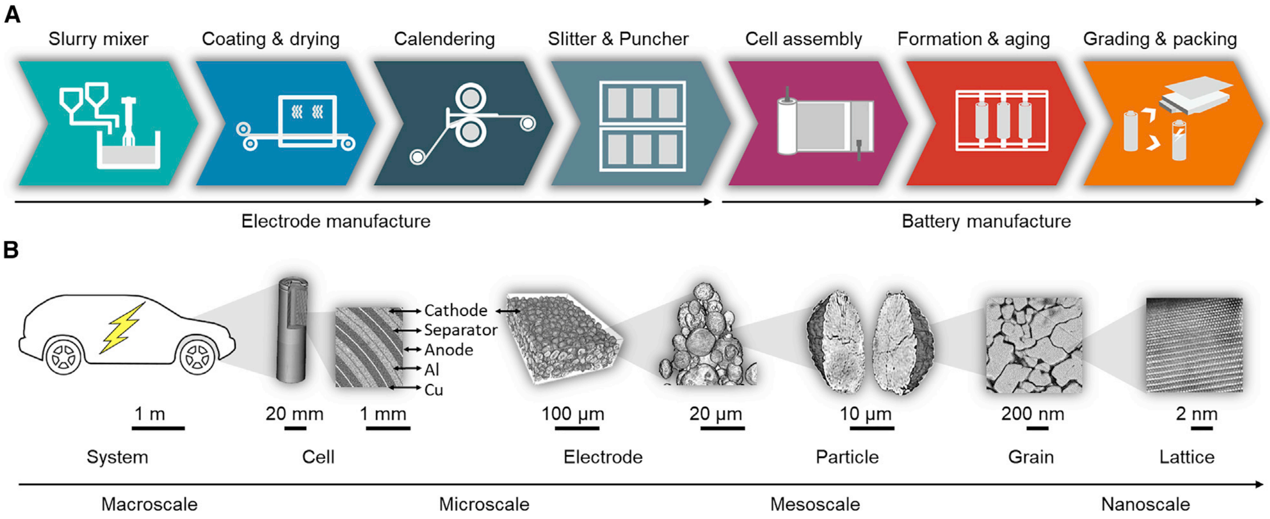

Figure 1. The complexity in commercial battery manufacture and multiscale morphology

(A) Schematic illustration of the industrial battery manufacturing process.

(B) The multiscale structural hierarchy of a Li-ion battery for electric vehicle application.

To improve the overall industrial LIB production yield and to make the QC process more effective and efficient, an in-depth understanding of the functional mechanisms of various structural defects in a LIB is essential. In particular, it is vitally important to discern different defect types, identify their respective sources and formation mechanisms, and understand their respective influences on the battery's state of health (SOH).[11–13] This knowledge can critically inform the battery production procedure with specifics on different manufacturing steps for minimizing different defects. It would also reduce the probability of having mildly defective cells slipping through the QC inspection due to the fact that their symptoms are rather unnoticeable in early stages of the battery lifetime, but could escalate in the practical operations involving temperature fluctuation and uneven current distribution.

In this work, a suite of state-of-the-art experimental techniques are applied to systematically investigate the defects in 18650-type cells structurally, chemically, and morphologically. Using multiscale X-ray tomography, we identify and visualize different structural defects in 18650-type cells that failed the routine assembly line QC inspection. After electrochemical cycles, we extract defective regions of interest from the 18650-type cells and conduct a suite of synchrotron-based comprehensive characterizations. In particular, we identify different impurity particles in the composite cathode and reveal their roles in the battery functionality. Our data suggest that the defect particles in the LIB cathode could affect the local chemistry directly through engaging in the redox reactions or indirectly through affecting the particles' self-assembling process. Our study gives insights on the nature of the chemical and morphological defects in LIBs, contributing to the improvement of the industry-scale battery manufacturing processes.

RESULTS

Identification of battery defects with X-ray microtomography

Since LIBs were first commercialized by Sony Corporation in the early 1990s,[14] the battery industry has been persistently putting in an immense effort to optimize and standardize the LIB manufacturing process. These efforts have significantly improved the product quality and production efficiency, thereby reducing the defect rate and the manufacturing cost. Figure 1A is a schematic overview of the

Please cite this article in press as: Qian et al., The role of structural defects in commercial lithium-ion batteries, Cell Reports Physical Science (2021), https://doi.org/10.1016/j.xcrp.2021.100554

industrial battery manufacturing procedure, which starts from the raw electrode material processing and goes all the way to the cell grading and battery pack assembling. Although this schematic seems straightforward, in practice, every single step in this workflow is highly intricate. Various structural and chemical defects can be induced into the battery, even if the practice of QC is rigorously executed. For example, a very mild tab burr could occur if the welding process is not perfect.[15] This tender defect can easily slip through the assembly line inspection. During prolonged battery operation, the tab burr could be incubated and become hazardous.[16] Another good example is the material's impurities, which are quite ubiquitous in many steps of the manufacturing workflow of the LIB.[13] The impurities could simply be inactive phases that have no significant functionality or become a seeding feature that provokes catastrophic cell damage during the cycling.

In addition to the sophistication in the LIB manufacturing process, the structure of the commercialized LIB for EV application is also highly complex, featuring a multiscale hierarchy, as illustrated using our data in Figure 1B. The desired cell-to-system level battery properties (e.g., excellent electrochemical performance, consistency, safety) are ultimately determined by the structural hierarchy of the battery. For example, the electrochemical redox heterogeneity,[17,18] mechanical robustness,[19,20] and the interplay among different structural components (e.g., active materials, conductive carbon, binder, the interconnected pore structure)[21] need to be addressed at the micro- (the electrode level) and the meso- (the particle level) scales. Fundamentally, the electrochemical cycling of a LIB concerns the diffusion of Li ions within and between the two composite electrodes. Therefore, the atomic-scale material properties (e.g., cation mixing,[22] strain,[20] lattice distortions,[23] crystal defects,[23] local phase transition[24]) have a very significant role to play in affecting the cell-level electrochemical performance. The hierarchical structural complexity of a LIB accentuates the need for an in-depth, multiscale, and multimodal experimental investigation. The present study is a good example of this kind.

We combined a suite of state-of-the-art X-ray microscopy and spectroscopy techniques to study a defective 18650-type cell that was singled out by the QC inspection process due to a problematic self-discharging effect[25] (see Figure S1). Starting at the macroscale, we studied the cell using X-ray computed tomography, which offers the capability of nondestructive three-dimensional (3D) imaging with multiscale spatial resolutions. In the studied cells, we captured several different structural defects as summarized in Figure 2. For example, the anode's Cu current collector is clearly deflected near the positive terminal of this cell (Figure 2A). We also observe the presence of burrs on the anode tab (Figure 2B). Randomly and sparsely distributed material impurities are observed in both cathode (Figure 2C) and anode (Figure 2D) electrodes. Finally, non-uniform active particle packing (Figure 2E) and electrode delamination (Figure 2F) are also detected by nano-resolution synchrotron tomography. All of these defects could profoundly influence the battery performance in practical applications. In this work, we chose to focus on the battery cathode and investigate the direct and indirect and immediate and long-term functional mechanisms for the impurities, which are ubiquitous and universal to LIB, regardless of the cell configuration.

Inspection of electrode defects with X-ray and Raman spectroscopy

As described above, we carried out microtomography measurements for a cell overview. Using these data, we identify and locate defective regions of interest within the 18650-type cylindrical LIB with $LiNi_{0.5}Co_{0.2}Mn_{0.3}O_2$ (NMC532) as the active cathode material and graphite as the anode. We purposely conducted an electrochemical

Please cite this article in press as: Qian et al., The role of structural defects in commercial lithium-ion batteries, Cell Reports Physical Science (2021), https://doi.org/10.1016/j.xcrp.2021.100554

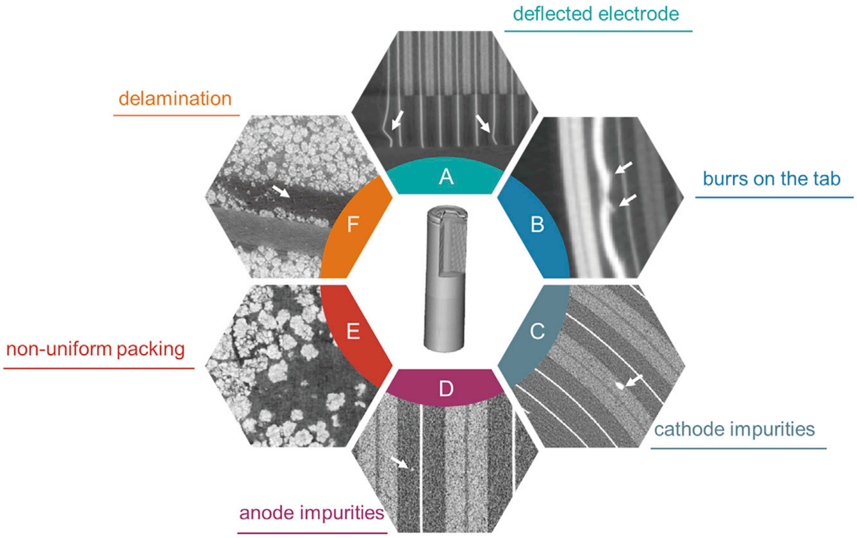

Figure 2. An overview of various structural defects in the commercial 18650-type Li-ion battery
(A) The deflected Cu current collector, an example of cell component deformation.
(B) Burrs on the tab.
(C and D) Examples of impurity particles in the cathode and anode, respectively.
(E and F) High-resolution visualizations of the defective electrode regions with non-uniform cathode packing and delamination, respectively.

cycling of the cell with a 1C/2C rate (Figures S2–S4). The cell was then charged to 4.2 V before it was disassembled in an Ar-filled glovebox. Based on the tomographic data, we located and cut out a few regions of 1 × 0.5 cm^2 from the unrolled electrode (Figures 3A and 3B). The harvested cathode samples were double-checked using microtomography to confirm their existence and to label the precise positions of the impurities and void defects (see Figure 3C). In the raw transmission image, the impurity is darker than the baseline area, suggesting that it is composed of high-Z elements with strong X-ray attenuation. To identify the chemical composition of these impurities, we conducted X-ray fluorescence (XRF) characterization with a focus on the identified defective particles within the field of view (FOV). Figure 3D illustrates the baseline XRF signal (associated with the normal area) and its peak fitting results. In addition to the anticipated transition metals, we observe signals of Ar and Au, which are from the atmosphere and instrument (the Au target). The K_α and K_β peaks of Mn, Co, and Ni between 5,900 and 8,267 eV were fitted with good fidelity, in good agreement with the nominal cathode composition (NMC532). We then compared this baseline spectrum to the signals coming from a few defective regions centered on the impurity particles (Figure 3E). It is interesting to note that there are mainly two types of impurities in terms of the chemical composition (Figure 3E). The first type is Fe/Cr-based particles, such as impurities #1 and #2, which contains elements that one could find in stainless steel. While some of them are exclusively made of Fe and Cr (#1 in Figure 3E), the others could contain additional metal elements (e.g., Cu and Zn; #2 in Figure 3E). Looking back at the battery manufacturing process, this type of impurity may originate from the raw material or from the instruments' abrasion during the manufacturing process. Another type of impurities are Zr-based particles (#3 in Figure 3E), which also show a trace of Hf. This type of impurity particle is likely zirconium oxide compounds, which may have been imported when zirconia milling balls were used during the production of the NMC cathode materials. It is useful to note that Zr doping is a broadly adopted method for improving the cathode performance.[26] Some residual Zr-based compounds could also be induced if the

Please cite this article in press as: Qian et al., The role of structural defects in commercial lithium-ion batteries, Cell Reports Physical Science (2021), https://doi.org/10.1016/j.xcrp.2021.100554

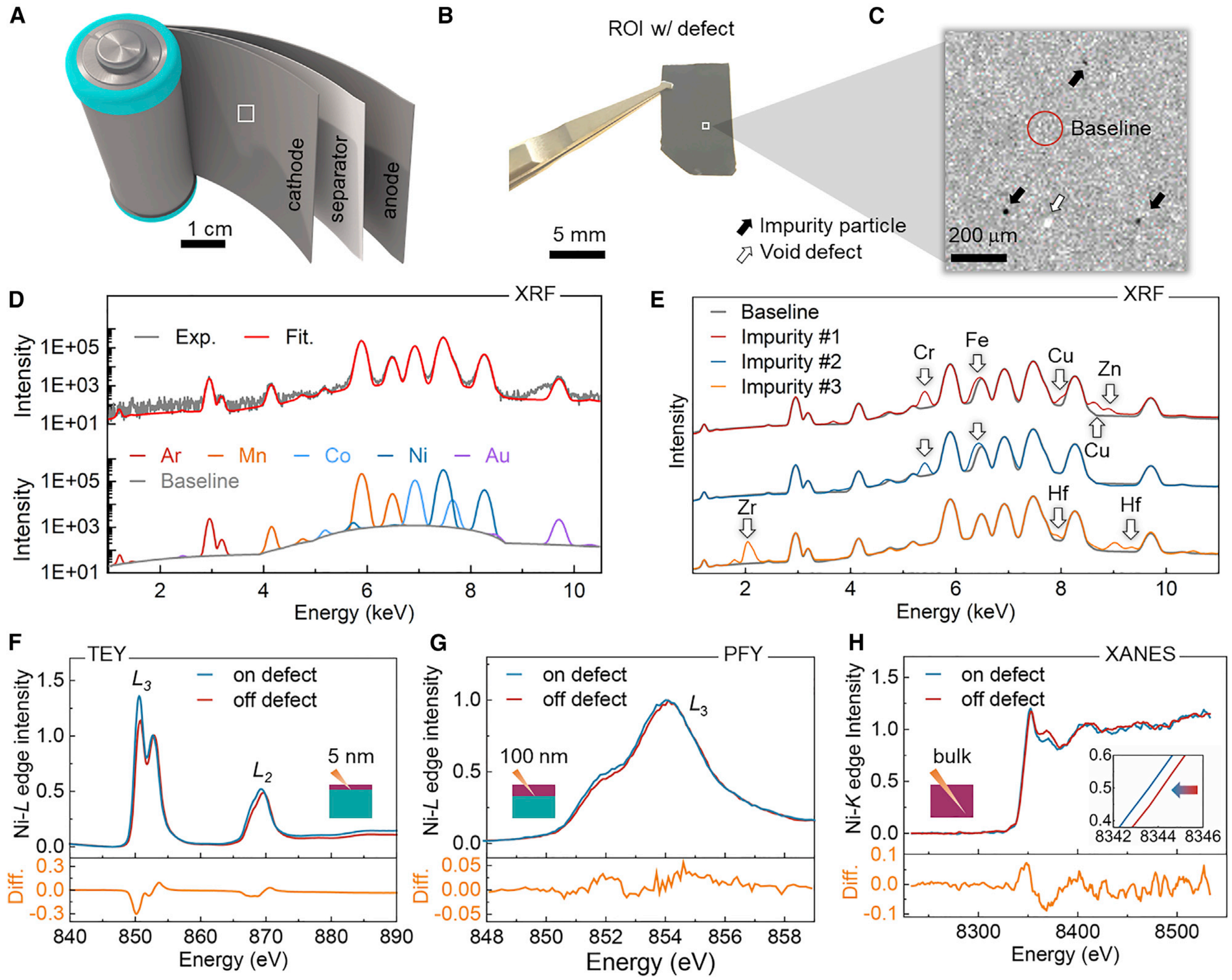

Figure 3. Schematic illustration of our experimental process for harvesting defective regions of interest from a 18650-type Li-ion battery

(A) Representation of the region of interest (ROI) extracted from the battery.

(B) The recovered ROI with defect particles.

(C) Micro-CT image of (B), in which the impurity and void defects are observed.

(D and E) The XRF analysis for the impurity defects with different chemical compositions on the detached cathode.

(F–H) The impact of defects on the cathode by depth-dependent absorption spectra analysis.

electrode manufacturing instruments were used for processing this type of material in the past.

To elucidate these impurity particles' functional mechanisms, depth-dependent synchrotron spectroscopy techniques were used to fingerprint the valence state of Ni near the defective regions (for #1 and #2 impurities, Fe/Cr-based particles). Here, we focus on the #1 and #2 impurities because they could be chemically active and, therefore, could have a more direct impact on the spectroscopic signature of Ni. The Zr-based #3 impurities, although they may not exhibit a direct chemical activity, could have an indirect impact, which we discuss later. Figures 3F and 3G show the soft X-ray absorption spectra, in total electron yield (TEY) and partial fluorescence yield (PFY) modes, centered on and away from the impurities in the 4.2-V charged cathode. The TEY offers an exceptional surface sensitivity, with the detected signal confined to an ~5-nm surface.[27] The PFY signal, however, can reach

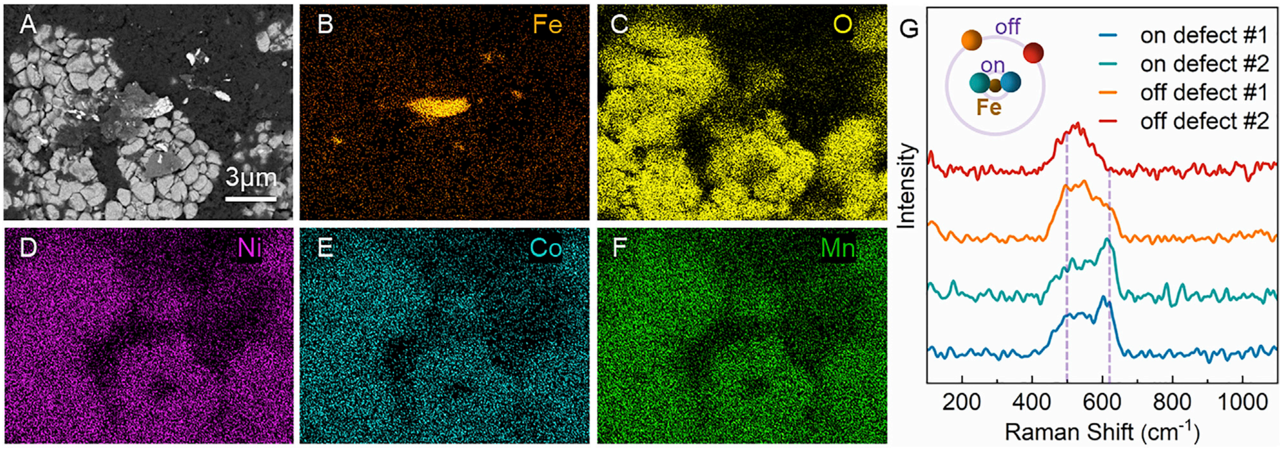

Figure 4. SEM-Raman characterization of the defective regions on NMC electrode

(A–F) The contrast imaging (A) and EDS mapping (B–F) of the defective regions.

(G) The Raman spectrum on and off defective regions. Blue and green profiles represent 2 different positions close to the defect; orange and red profiles represent 2 different positions far away from the defect.

up to ~100 nm in depth, covering some sub-surface chemical information.[28,29] We note here that a superconducting transition edge sensor (TES) detector was used in our fluorescence yield measurements, which allows us to reject unwanted phonons for suppressing the self-absorption induced spectrum distortion.[28] In our data, the L_3 edge of Ni splits into two peaks with competing intensities, representing the relative concentration of low-valence Ni and high-valence Ni, respectively. The TEY signal shows a lower valence Ni on the defective area, suggesting an enhanced lattice reconstruction effect[27] (from layered to spinel and/or rock salt structures) near the #1 and #2 impurities. A similar tendency also appeared in the PFY data. Since the PFY probes up to 100 nm into the electrode surface, it is a mixture of surface signal and subsurface chemistry. The fact that the PFY signal over the defective region shows a slightly reduced Ni valence could be attributed to a combined effect of the surface reconstruction and the reduction of the bulk Ni due to a charge transfer between the active cathode material and the impurity particles. To further amplify the bulk signal, hard X-ray near-edge absorption spectroscopy (XANES) measurements were conducted in the transmission mode. The XANES data shown in Figure 3H confirm that the bulk Ni is slightly reduced in the defective regions, as it is indicated by the >0.5 eV shift of the XANES spectrum (see inset in Figure 3H). These depth-dependent spectroscopic investigations clearly suggest that the Fe/Cr-based impurities are chemically active. They affect the local Ni valence state by affecting the degree of surface reconstruction and by inducing a local discharging of the NMC cathode, thereby exacerbating the local electrochemical redox heterogeneity.

To further support the above inference, scanning electron microscopy (SEM)-Raman measurements were performed, and the results are shown in Figure 4. By large FOV energy-dispersive X-ray spectroscopy (EDS) mapping (Figure S5), we detect a specific impurity particle cluster centered around an Fe particle of ~3 μm on the electrode. We observe a strong Fe signal and weak signals for O, Ni, Co, and Mn, which suggests that it is a metallic Fe cluster rather than Fe oxides (see Figures 4A–4F and S6). Due to the adverse effect of the presence of Fe-based impurities (Figure S7), we evaluated its impact on the local NMC particles by conducting Raman spectroscopy with a focused laser probe. The "on defect" Raman spectrum is collected with the laser beam centered on a Fe-rich spot, while the regions without any impurity signals are called "off defect."

We sampled many different locations, and the representative spectra are shown in Figures 4G and S8. Compared to the spectrum collected at off defect positions, the on defect spectra show decreased peak intensity at ~490 cm^{-1} and a new peak at ~610 cm^{-1}. These Raman features imply that there is a higher concentration of Li in the NMC particle near the Fe impurities, indicating a local discharging effect.[30] As revealed by the SEM image, the large Fe particle at the cluster center features a rather irregular shape and is located near the cathode-to-separator interface. It has the potential to trigger micro-short circuit because the multilayer structure is rather compact and would swell during the electrochemical cycling.

Visualization of electrode defects with X-ray nanotomography

We further investigate the micromorphology of the NMC composite cathode using nano-resolution holographic X-ray computed tomography (HXCT). We carried out this measurement over several regions with and without the above-discussed structural defects (e.g., impurity particles). Figure 5A shows a randomly selected 3D rendering of an impurity-free region recovered from a defective 18650-type Li-ion battery. After quantitative phase retrieval and tomographic reconstruction, the gray level of the voxels is directly proportional to the local electron density. The bright gray materials are the NMC particles, whereas the dark gray regions represent the conductive and porous carbon-binder domain (CBD). The irregularly shaped NMC particles at ~4–5 μm exhibit a very different degree of cracking, as shown in the virtual slice in Figures 5B and 5C, with the undamaged particles labeled with red contours. The structural disintegration of the NMC particle not only deteriorates the electric conductivity and the mechanical stiffness of the electrode but also facilitates the infiltration of the liquid electrolyte along the interconnected cracks and aggravates the undesired surface degradation. In addition to the heterogeneous particle cracking, our data on the defective electrodes show several different types of impurities, as presented in Figures 5D–5F. Figure 5D shows a large spherical NMC particle embedded in the electrode. While the composition of this large NMC particle is very similar to the other active cathode particles in the electrode, it demonstrates a clear and substantial impact on the local particle assembly. This is related to the self-assembly process of the cathode particles during the drying of the slurry, which is a dynamic and highly complicated process that entails delicate control of the electrode solidification conditions.[31] A similar effect can be observed in Figure 5F, which centers on a Zr-based large impurity particle (see Figure S9 for the XRF mapping and fitting results). In Figure 4E, however, even though a Zr-based particle does exist, it was not capable of causing the particles to change their self-assembly behavior due to its small size and limited mass. The heterogeneity in the local packing density of the active materials could escalate the charge heterogeneity in the electrode, which leads to different degrees of electrode utilization upon battery cycling. The defective regions may also exhibit unbalanced electron and ion conductivity, causing local over-charging/discharging and deactivation. To qualify the uniformity of the active particle packing, we calculate the spatial distribution of the porosity over the regions that correspond to Figures 5D and 5E (see Figures 5G and 5H, respectively). Visual assessment suggests that Figure 5G has a larger color variation in comparison with Figure 5H, suggesting that the packing density is more heterogeneous in the presence of large impurity particle(s). This observation is further quantified in Figure 5I by showing the probability and the spread of the local packing density value around the particles in Figures 5D and 5E. Affected by the presence of a large particle, the local porosity distribution exhibits a lower value and a higher variation.

DISCUSSION

Although the consensus is that the ubiquitous structural and chemical defects in a LIB are functionally very important, their functional mechanisms are not well

Please cite this article in press as: Qian et al., The role of structural defects in commercial lithium-ion batteries, Cell Reports Physical Science (2021), https://doi.org/10.1016/j.xcrp.2021.100554

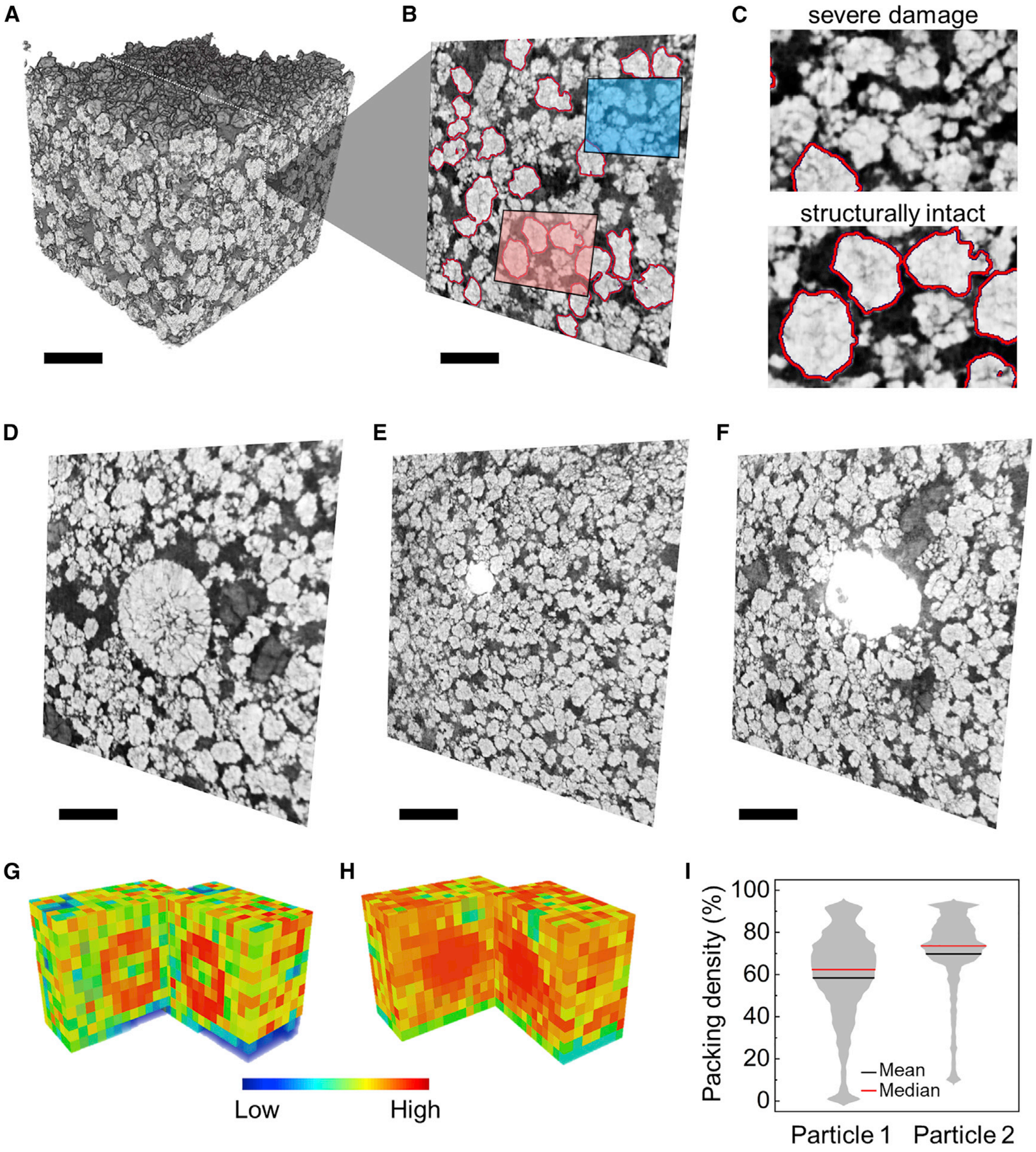

Figure 5. Nanoresolution X-ray holotomography of NMC composite cathode recovered from a defective 18650-type Li-ion battery cell

(A–C) (A) 3D rendering of a randomly selected region, with its central slice shown in (B) and 2 ROIs with different degrees of damage enlarged in (C). The scar bar in (A) and (B) are 8 and 5 μm, respectively.

(D–F) Regions with various types of defect particles. Scale bar, 5 μm.

(G and H) The packing density around particles with abnormal and normal sizes, respectively.

(I) Representation of the packing density around an abnormal-size particle (particle 1) and a regular size particle (particle 2).

understood. In this study, we investigate the defects in commercial 18650-type LIB using a suite of cutting-edge X-ray tomography, SEM-Raman spectroscopy, and synchrotron-based analytical techniques. Based on our multiscale and comprehensive experiments, we summarize our observations and interpret the degradation mechanisms associated with the presence of impurities in the battery (see Figure 6). Depending on the composition, the metallic impurities can be directly involved in the chemical reactions. They could alter the surface chemistry and

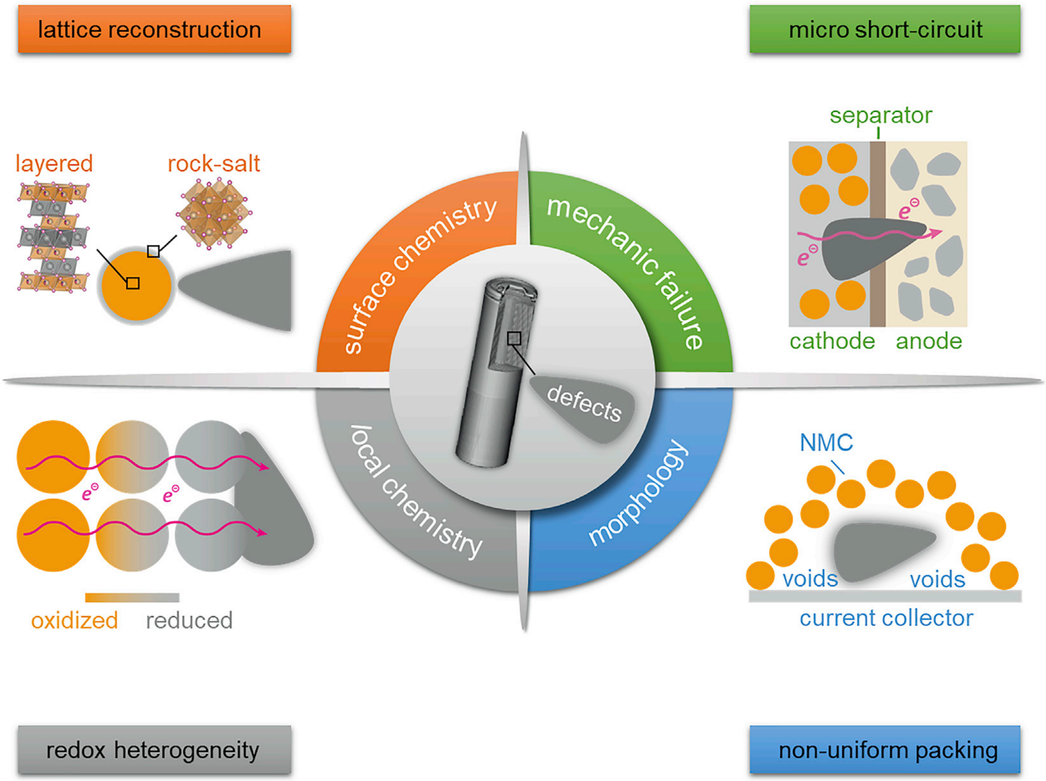

Figure 6. A schematic illustration of the functional mechanisms of the battery defects concluded from our study

The presence of defect particles in the 18650 cells could lead to multiscale degradations, for example, at the active particle level (lattice reconstruction), the electrode level (redox heterogeneity and non-uniform packing), and the battery level (micro-short circuit).

intensify the surface reconstruction effect of the NMC particles, leading to an increased electrochemical impedance and polarization. These impurities can also engage in the redox reactions in the bulk at the electrode level. Local electrochemical redox heterogeneity can be further exacerbated, which could, in turn, accelerate the electrode degradation. If the impurities are located near the separator (see Figure S10), then the risk of internal short circuit will be significantly amplified because these conductive particles could pierce through the separator. Once established, the internal short circuit will induce a large local current and provoke a thermal runaway. To prevent such problems, it is important to reinforce the QC throughout the LIB production procedure. Examples include choosing high-quality raw materials with good purity, reducing dust and equipment abrasion during fabrication, and enhancing the capability of removing magnetic impurities.

Besides impurities, non-uniform active particle packing is another common form of morphological defect in the LIB electrode. This type of defect can easily appear in the electrode when particles with distinct sizes coexist. Particle packing at the electrode level plays a significant role in affecting the lifetime of the battery. Poor mechanic robustness and deactivation of NMC particles due to contact failure will arise in the presence of non-uniform packing. It is worth noting that mixing active cathode particles of different sizes (e.g., blending polycrystal and single-crystal NMC particles) has been explored as an effective approach to improve the overall performance

Please cite this article in press as: Qian et al., The role of structural defects in commercial lithium-ion batteries, Cell Reports Physical Science (2021), https://doi.org/10.1016/j.xcrp.2021.100554

of the electrode. Our results suggest that the coexistence of particles of very different sizes could cause complexities in the self-assembling process, and this approach shall be adopted with caution. To conclude, a comprehensive understanding of the structural and chemical defects of the LIB and their functional mechanisms constitutes a research front that is of both scientific and industrial significance. Our systematic investigation offers valuable insights for improving the industrial LIB manufacturing processes.

EXPERIMENTAL PROCEDURES

Resource availability

Lead contact

Further information and requests for resources should be directed to and will be fulfilled by the lead contact, Yijin Liu (liuyijin@slac.stanford.edu).

Materials availability

This study did not generate new unique materials. The full details of all of the experiments and materials are provided in the supplemental information.

Data and code availability

The source code relevant to this study are available at https://github.com/SSRL-LiuGroup.

SUPPLEMENTAL INFORMATION

Supplemental information can be found online at https://doi.org/10.1016/j.xcrp.2021.100554.

ACKNOWLEDGMENTS

This work at the Stanford Synchrotron Radiation Lightsource, SLAC National Accelerator Laboratory, is supported by the US Department of Energy (DOE), Office of Science, Office of Basic Energy Sciences under contract no. DE-AC02-76SF00515. This work is also supported by a junior faculty start-up grant of Shanghai Jiao Tong University (to L.L.), the Natural Science Foundation of China (22008154, to L.S.L., 2167165, to Z.-F.M.), and in part by SINOPEC (420038-1, to L.L). The work at IOP was supported by funding from the Natural Science Foundation of Beijing (grant no. Z20J00042) and Newton Advanced Fellowships. Sigray gratefully acknowledges funding from the Department of Health and Human Services of the National Institutes of Health under grant nos. R44GM133287 and R43GM112413. This research used the nanoresolution HXCT beamline at the Nano-Imaging beamline ID16A-NI at the ESRF, Grenoble, France. The engineering support of D. Van Campen, D. Day, and V. Borzenets for the TXM experiment at beamline 6-2C of SSRL is gratefully acknowledged.

AUTHOR CONTRIBUTIONS

Y.L., L.L., X.Y., and P.C. conceived this study. G.Q. and D.M. performed the electrochemical tests and electrode sample preparation. D.M. and G.Q. performed the SEM-Raman measurements. D.M., G.Z., S.G., D.V., and B.S. performed the micro-computed tomography (CT) and micro-XRF tests. G.Q., S.-J.L., and J.-S.L. carried out the soft XAS and resonant inelastic X-ray scattering (RIXS) measurements. J.Z. and G.Q. performed the XANES measurements and analysis. F.M., D.K., P.C., J.L., and Y.L. conducted the nanotomography tests and analysis. Z.-F.M., W.Y., P.P., X.Y., L.L., P.C., and Y.L. contributed to the scientific interpretation of the data. G.Q., F.M., D.M., and Y.L. wrote the manuscript, with assistance from all of the coauthors.

Please cite this article in press as: Qian et al., The role of structural defects in commercial lithium-ion batteries, Cell Reports Physical Science (2021), https://doi.org/10.1016/j.xcrp.2021.100554

DECLARATION OF INTERESTS

The authors declare no competing interests.

Received: April 10, 2021
Revised: July 19, 2021
Accepted: August 5, 2021
Published: August 25, 2021

REFERENCES

1. Cano, Z.P., Banham, D., Ye, S., Hintennach, A., Lu, J., Fowler, M., and Chen, Z. (2018). Batteries and fuel cells for emerging electric vehicle markets. Nat. Energy *3*, 279–289.
2. Zeng, X., Li, M., Abd El-Hady, D., Alshitari, W., Al-Bogami, A.S., Lu, J., and Amine, K. (2019). Commercialization of Lithium Battery Technologies for Electric Vehicles. Adv. Energy Mater. *9*, 1900161.
3. Arora, S., Kapoor, A., and Shen, W. (2018). Application of Robust Design Methodology to Battery Packs for Electric Vehicles: Identification of Critical Technical Requirements for Modular Architecture. Batteries *4*, 30.
4. Xiong, R., Li, L., and Tian, J. (2018). Towards a smarter battery management system: a critical review on battery state of health monitoring methods. J. Power Sources *405*, 18–29.
5. Rahimi-Eichi, H., Ojha, U., Baronti, F., and Chow, M. (2013). Battery Management System: An Overview of Its Application in the Smart Grid and Electric Vehicles. IEEE Ind. Electron. Mag. *7*, 4–16.
6. Gallardo-Lozano, J., Romero-Cadaval, E., Milanes-Montero, M.I., and Guerrero-Martinez, M.A. (2014). Battery equalization active methods. J. Power Sources *246*, 934–949.
7. Finegan, D.P., Scheel, M., Robinson, J.B., Tjaden, B., Hunt, I., Mason, T.J., Millichamp, J., Di Michiel, M., Offer, G.J., Hinds, G., et al. (2015). In-operando high-speed tomography of lithium-ion batteries during thermal runaway. Nat. Commun. *6*, 6924.
8. Feng, X., Ouyang, M., Liu, X., Lu, L., Xia, Y., and He, X. (2018). Thermal runaway mechanism of lithium ion battery for electric vehicles: a review. Energy Storage Mater. *10*, 246–267.
9. Wang, Q., Ping, P., Zhao, X., Chu, G., Sun, J., and Chen, C. (2012). Thermal runaway caused fire and explosion of lithium ion battery. J. Power Sources *208*, 210–224.
10. Juarez-Robles, D., Vyas, A.A., Fear, C., Jeevarajan, J.A., and Mukherjee, P.P. (2020). Overcharge and Aging Analytics of Li-Ion Cells. J. Electrochem. Soc. *167*, 090547.
11. Mohanty, D., Hockaday, E., Li, J., Hensley, D.K., Daniel, C., and Wood, D.L. (2016). Effect of electrode manufacturing defects on electrochemical performance of lithium-ion batteries: cognizance of the battery failure sources. J. Power Sources *312*, 70–79.
12. Günther, T., Schreiner, D., Metkar, A., Meyer, C., Kwade, A., and Reinhart, G. (2020). Classification of Calendering-Induced Electrode Defects and Their Influence on Subsequent Processes of Lithium-Ion Battery Production. Energy Technol. (Weinheim) *8*, 1900026.
13. Wu, Y., Saxena, S., Xing, Y., Wang, Y., Li, C., Yung, W.K.C., and Pecht, M. (2018). Analysis of Manufacturing-Induced Defects and Structural Deformations in Lithium-Ion Batteries Using Computed Tomography. Energies *11*, 925.
14. Ozawa, K. (1994). Lithium-ion rechargeable batteries with $LiCoO_2$ and carbon electrodes: the $LiCoO_2$/C system. Solid State Ion. *69*, 212–221.
15. Yao, X., and Pecht, M.G. (2019). Tab Design and Failures in Cylindrical Li-ion Batteries. IEEE Access *7*, 24082–24095.
16. Yao, X., Saxena, S., Su, L., and Pecht, M.G. (2019). The Explosive Nature of Tab Burrs in Li-Ion Batteries. IEEE Access *7*, 45978–45982.
17. Xu, Z., Jiang, Z., Kuai, C., Xu, R., Qin, C., Zhang, Y., Rahman, M.M., Wei, C., Nordlund, D., Sun, C.-J., et al. (2020). Charge distribution guided by grain crystallographic orientations in polycrystalline battery materials. Nat. Commun. *11*, 83.
18. Tian, C., Xu, Y., Nordlund, D., Lin, F., Liu, J., Sun, Z., Liu, Y., and Doeff, M. (2018). Charge Heterogeneity and Surface Chemistry in Polycrystalline Cathode Materials. Joule *2*, 464–477.
19. Yang, Y., Xu, R., Zhang, K., Lee, S.-J., Mu, L., Liu, P., Waters, C.K., Spence, S., Xu, Z., Wei, C., et al. (2019). Quantification of Heterogeneous Degradation in Li-Ion Batteries. Adv. Energy Mater. *9*, 1900674.
20. Xu, Z., Rahman, M.M., Mu, L., Liu, Y., and Lin, F. (2018). Chemomechanical behaviors of layered cathode materials in alkali metal ion batteries. J. Mater. Chem. A Mater. Energy Sustain. *6*, 21859–21884.
21. Jiang, Z., Li, J., Yang, Y., Mu, L., Wei, C., Yu, X., Pianetta, P., Zhao, K., Cloetens, P., Lin, F., and Liu, Y. (2020). Machine-learning-revealed statistics of the particle-carbon/binder detachment in lithium-ion battery cathodes. Nat. Commun. *11*, 2310.
22. Zheng, J., Ye, Y., Liu, T., Xiao, Y., Wang, C., Wang, F., and Pan, F. (2019). Ni/Li Disordering in Layered Transition Metal Oxide: Electrochemical Impact, Origin, and Control. Acc. Chem. Res. *52*, 2201–2209.
23. Hong, Y.-S., Huang, X., Wei, C., Wang, J., Zhang, J.-N., Yan, H., Chu, Y.S., Pianetta, P., Xiao, R., Yu, X., et al. (2020). Hierarchical Defect Engineering for $LiCoO_2$ through Low-Solubility Trace Element Doping. Chem *6*, 2759–2769.
24. Qian, G., Zhang, Y., Li, L., Zhang, R., Xu, J., Cheng, Z., Xie, S., Wang, H., Rao, Q., He, Y., et al. (2020). Single-crystal nickel-rich layered-oxide battery cathode materials: synthesis, electrochemistry, and intra-granular fracture. Energy Storage Mater. *27*, 140–149.
25. Deutschen, T., Gasser, S., Schaller, M., and Siehr, J. (2018). Modeling the self-discharge by voltage decay of a NMC/graphite lithium-ion cell. J. Energy Storage *19*, 113–119.
26. Qian, G., Huang, H., Hou, F., Wang, W., Wang, Y., Lin, J., Lee, S.-J., Yan, H., Chu, Y.S., Pianetta, P., et al. (2021). Selective dopant segregation modulates mesoscale reaction kinetics in layered transition metal oxide. Nano Energy *84*, 105926.
27. Lin, F., Nordlund, D., Markus, I.M., Weng, T.-C., Xin, H.L., and Doeff, M.M. (2014). Profiling the nanoscale gradient in stoichiometric layered cathode particles for lithium-ion batteries. Energy Environ. Sci. *7*, 3077–3085.
28. Li, S., Lee, S.-J., Wang, X., Yang, W., Huang, H., Swetz, D.S., Doriese, W.B., O'Neil, G.C., Ullom, J.N., Titus, C.J., et al. (2019). Surface-to-Bulk Redox Coupling through Thermally Driven Li Redistribution in Li- and Mn-Rich Layered Cathode Materials. J. Am. Chem. Soc. *141*, 12079–12086.
29. Lee, S.-J., Titus, C.J., Alonso Mori, R., Baker, M.L., Bennett, D.A., Cho, H.-M., Doriese, W.B., Fowler, J.W., Gaffney, K.J., Gallo, A., et al. (2019). Soft X-ray spectroscopy with transition-edge sensors at Stanford Synchrotron Radiation Lightsource beamline 10-1. Rev. Sci. Instrum. *90*, 113101.
30. Flores, E., Novák, P., and Berg, E.J. (2018). In situ and Operando Raman Spectroscopy of Layered Transition Metal Oxides for Li-ion Battery Cathodes. Front. Energy Res. *6*, 82.
31. Yang, Y., Xu, Z., Steiner, J.D., Liu, Y., Lin, F., and Xiao, X. (2020). Quantitative probing of the fast particle motion during the solidification of battery electrodes. Appl. Phys. Lett. *116*, 081904.